JOURNAL OF AGRICULTURAL AND FOOD CHEMISTRY

Article

pubs.acs.org/JAFC

Adsorption and Desorption Properties of Macroporous Resins for Anthocyanins from the Calyx Extract of Roselle (*Hibiscus sabdariffa* L.)

Xiu-Lian Chang,[†] Dong Wang,[†] Bi-Yun Chen,[†] Yong-Mei Feng,[†] Shao-Hong Wen,*[,†] and Peng-Yuan Zhan[§]

[†]School of Life Sciences, Yantai University, Yantai 264005, People's Republic of China

[§]Qindao Pengyuan Kanghua Natural Products Company, Ltd., Laixi 266600, People's Republic of China

ABSTRACT: Adsorption of roselle anthocynins, a natural pigment, onto various macroporous resins was optimized to develop a simple and efficient process for industrial separation and purification of roselle anthocyanins. Nine different macroporous resins (AB-8, X-5, HPD-100, SP-207, XAD-4, LS-305A, DM-21, LS-610B, and LS-305) were evaluated for the adsorption properties of the anthocyanins extracted from the calyx extract of *Hibiscus sabdariffa* L. The influences of phase contact time, solution pH, initial anthocyanin concentration, and ethanol concentration with different citric acid amounts were studied by the static adsorption/desorption method. The adsorption isotherm data were fitted well to the Langmuir isotherm, and according to this model, LS-610B and LS-305 exhibited the highest monolayer sorption capacities of 31.95 and 38.16 mg/g, respectively. The kinetic data were modeled using pseudo-first-order, pseudo-second-order, and intraparticle diffusion equations. The experimental data were well described by the pseudo-second-order kinetic model. Continuous column adsorption−regeneration cycles indicated negligible capacity loss of LS-305 during operation. The overall yield of pigment product was 49.6 mg/g dried calyces. The content of roselle anthocynins in the pigment product was 4.85%.

KEYWORDS: *anthocyanins, Hibiscus sabdariffa L., calyx extract, adsorption, desorption, macroporous resin*

INTRODUCTION

Roselle (*Hibiscus sabdariffia* L.) is a tropical plant of considerable economic potential. Its calyces have been suggested for the production of soft drinks, roselle tea, jam, juices, and natural food colorants.[1−3] The calyces are rich in anthocyanins, ascorbic acid, organic acids, flavonoids, and polyphenols.[3,4] Recent research shows that anthocyanin is the major source of antioxidant capacity in roselle extract.[5−7] It is used effectively in folk medicines for the treatment of hypertension, inflammatory diseases and cancer, heart and nerve disorders, high blood pressure, and calcified arteries.[4,8] Roselle anthocyanins were identified as having delphinidin-3-sambubioside (70% of the anthocyanins) and cyanidin-3-sambubioside as the major pigments, with delphinidin-3-glucoside and cyanidin-3-glucoside as the minor ones.[9,10]

The concentration of roselle extracts, through osmotic evaporation concentration,[11] ultrafiltration and nanofiltration, and membrane concentration,[12] has been reported recently. However, concentration can only give a mixture of anthocyanins, organic acids, carbohydrates, etc., not a relatively pure anthocyanin product. Macroporous resins, because of their relatively low cost and easy regeneration, have been employed in the purification of several anthocyanins, including cyanidin 3-glucoside,[13] anthocyanins from citrus-processing byproducts,[14] anthocyanins from blood oranges,[15] and anthocyanins from black currant fruits.[16] Tsai et al.[5] first reported the purification of roselle anthocyanin extract using Amberlite XAD-2 macroporous resin and HPLC aimed at studying the antioxidant activity of roselle anthocyanins, without screening of optimum resin.

In the present study, nine macroporous resins selected according to the resin manufacturer's recommendation and in accordance with current good manufacturing practice by our cooperative production unit (Qindao Pengyuan Kanghua Natural Products Co., Ltd., China) were used to systematically investigate the adsorption and desorption of anthocyanins from roselle calyx extract and to develop a simple and efficient process for the preliminary separation and purification of roselle anthocyanins with the optimal resin.

MATERIALS AND METHODS

Materials. Dry calyces of roselle (*H. sabdariffa* L.) were kindly supplied by Zhangzhou Gold Saga Biotechnology Co., Ltd., China. All reagents were of analytical grade.

The resin XAD-4 was purchased from Rohm & Haas, USA. Diaion SP-207 was from Mitsubishi Chemical Industries, Japan. X-5 and AB-8 were purchased from the Chemical Plant of Nankai University, China. LS-610B, LS-305, and LS-305A were from Shaanxi Lanshen Special Resin Co., Ltd., China. HPD-100 was from Anhui Sanxing Resin Technology Co., Ltd., China. DM-21 was from Shandong Lukang Record Pharmaceuticals Co., Ltd., China. All resins are made of styrene−divinylbenzene.

Preparation of Extracts. Dry calyces of roselle were extracted with deionized water using a mass ratio of calyx to water of 1:15 for 1.5 h at 60 °C. The extraction procedure was repeated three times, until the extract was colorless. The extracts were combined and filtered

Received: December 26, 2011
Revised: February 12, 2012
Accepted: February 13, 2012
Published: February 13, 2012

Table 1. Characteristics of the Adsorbent Resins Used and Their Adsorption Properties on Roselle Anthocyanins

type	polarity	surface area (m^2/g)	pore size (Å)	adsorption capacity, q_e (mg/g)	desorption ratio, D (%)
AB-8	semipolar	480−520	130−140	6.12 ± 0.26	94.21 ± 2.13
X-5	apolar	500−600	290−300	10.59 ± 0.34	93.31 ± 2.09
HPD-100	apolar	650−700	85−90	15.56 ± 0.31	94.39 ± 1.84
SP-207	apolar	600	110	20.03 ± 0.46	94.66 ± 3.75
DM-21	apolar	1000	50−60	21.98 ± 0.25	95.15 ± 2.86
LS-305A	apolar	850−950	80	22.25 ± 0.44	89.89 ± 2.97
LS-610B	apolar	950−1050	55	22.94 ± 0.58	84.54 ± 2.59
LS-305	apolar	900−1000	60	23.16 ± 0.62	90.34 ± 1.68
XAD-4	apolar	750	100	23.34 ± 0.49	55.09 ± 1.79

through a filter paper, then concentrated under reduced pressure with a rotary evaporator (RE-52A, Shanghai Yarong Biochemical Factory, Shanghai, China), and then kept at 4 °C until used.

Determination of Roselle Anthocyanin Content. Data indicated that the absorption maximum of the water extract of roselle anthocyanins was found to be at wavelength of 520 nm. The same result was reported in the literature.[3,17,18]

The roselle anthocyanin content was determined by the pH differential method.[19] A Spectrumlab 752s UV−vis spectrophotometer (Shanghai Lengguang Technology Co. Ltd., Shanghai, China) was used for spectral measurements at 520 and 700 nm, respectively, using deionized water as a blank. The difference in absorbance values at pH 1.0 and 4.5 was directly proportional to the concentration of roselle monomeric anthocyanins, which was calculated on the basis of delphinidin 3,5-sumboside, with a molecular weight of 577 g/mol and a molar absorption coefficient of 26000 L mol^{-1} cm^{-1}.[20,21]

Pretreatment of Macroporous Resins. Prior to use, the macroporous resins were leached with 95% ethanol for 24 h and washed several times with deionized water. Subsequently, the resins were soaked in 1 M NaOH for 5 h and then washed by distilled water. The washed resins were soaked in 1 M HCl for 5 h. Finally, the resins were washed by distilled water thoroughly. Their surface moisture was removed by pressing gently between the folds of filter paper (termed filter paper dried (FPD) resin). The FPD resins were immediately packed in nylon bags sealed with an impulse sealer and kept in a styrofoam box until used. The dry-basis weight of sorbent was measured by weighing the sorbent particles after drying for 12 h at 80 °C. In all adsorption studies the resin used was FPD resin. All calculations are done on the basis of dry resin.

Preselection of Resins. The preselection of resins was evaluated by their adsorption capacities and desorption ratios. All adsorbents (Table 1) were investigated as follows: a preweighed amount of FPD resins (equal to 1.0 g of dry resin) and 40 mL of crude extract solution with initial concentration of 608.07 mg/L at pH 2.80 were added into each flask with a lid. The flasks were shaken on a shaker (100 rpm) at 25 °C for 24 h. The solution after adsorption was analyzed using the UV−vis spectrophotometer.

Desorption experiments were conducted as follows: after the attainment of adsorption equilibrium, the absorbed resins were filtered through a 200 mesh screen and then added with 20 mL of 65% ethanol solution containing 3 g/L citric acid into each flask with a lid. The flasks were shaken on a shaker (100 rpm) at 25 °C for 24 h.

The adsorption capacity of the resins, q_e (mg/g), was calculated according to the following equation:

$$q_e = \frac{(C_0 - C_e)}{W} \times V \quad (1)$$

The desorption ratio of the resin, D (%), was calculated according to the equation

$$D = \frac{C_d V_d}{(C_0 - C_e) \times V} \times 100\% \quad (2)$$

where C_0 and C_e are the initial and equilibrium liquid-phase concentrations (mg/L), respectively, V is the volume of solution (L), and W is the weight of dry resins (g). C_d and V_d are the concentration of roselle anthocyanins in desorption solution (mg/L) and the volume (L), respectively.

Adsorption Isotherm Experiments. Adsorption equilibrium data were obtained by introducing a preweighed amount of FPD resin (equal to 0.2 g of dry resin) into 20 mL of crude extract solution at different initial concentrations of roselle anthocyanins (88.4, 176.8, 265.2, 353.6, 442.0, and 530.4 mg/L) at different initial pH values (pH 2.0, 2.5, and 3.0) adjusted by concentrated hydrochloric acid and 1 M NaOH solutions, and shaking at 100 rpm at 25 °C for 24 h.

Desorption Experiments. Preweighed amounts of four selected FPD resins, LS-305, LS-305A, LS-610B, and D-M21 (equal to 5.0 g of dry resin), were added into 200 mL of crude extract solution at the initial concentration of 543.71 mg/L at pH 2.5, followed by shaking at 100 rpm at 25 °C for 24 h. After the attainment of adsorption equilibrium, the adsorbed resins were washed with distilled water and then dried by filter paper as described under Pretreatment of Macroporous Resins. Preweighed amounts of four adsorbed FPD resins (equal to 0.25 g of dry unadsorbed resin) and 10 mL of different ethanol solution (50, 60, 70, 80, and 95%) containing various citric acid concentrations (0, 1.5, 3, and 4.5 g/L) were added into each flask with a lid, followed by shaking at 100 rpm at 25 °C for 24 h and measuring the concentration of roselle anthocyanins in the desorption solution.

Static Adsorption and Desorption Kinetics. The adsorption kinetics of the selected macroporous resin was studied by contacting 50 mL of crude exaction solution (pH 2.5, initial concentration = 639.14 mg/L) with a preweighed amount of hydrated resins (equal to 0.5 g of dry resin) on a shaker (100 rpm) at 25 °C. The concentration of roselle anthocyanins in the adsorption solution was determined at different times until equilibration.

After the attainment of adsorption equilibrium, the absorbed resins were filtered through a 200 mesh screen and then added with 25 mL of a 60% ethanol aqueous solution with 3 g/L citric acid into each flask with a lid. The flasks were shaken on a shaker (100 rpm) at 25 °C. The concentration of roselle anthocyanins in the desorption solution was determined at different times.

Dynamic Adsorption and Elution Experiments. The separation properties of the three selected resins, LS-305, LS610B, and DM-21, were evaluated by the dynamic tests.

Dynamic adsorption tests were carried out as follows: the hydrated adsorbent was packed into a glass column (50 cm × 1 cm) with a bed volume (BV) of 40 mL. The sample solution was introduced downward into the column, and then the adsorbent column was rinsed by 3 BV of deionized water. The concentration of anthocyanins in the exit solution was analyzed by the UV−vis spectrophotometer.

Breakthrough adsorption capacity and saturation capacity were calculated on the basis of the amount of anthocyanins adsorbed when the concentration of the exit from the column reached 5 and 95% of the inlet solution concentration, respectively. The adsorption capacity q (mg/mL resin) was calculated with eq 3[22,23]

$$q = \frac{V_s(C_i - C_a)}{V_w} \quad (3)$$

dx.doi.org/10.1021/jf205311v | J. Agric. Food Chem. 2012, 60, 2368−2376

where C_i is the concentration of initial solution (mg/L), C_a is the average concentration of the effluent (mg/L), V_s is the volume of sample solution (L), and V_w is the volume of wet resin (mL).

A dynamic desorption test was performed as follows: the adsorbate-laden column was desorbed by 60% ethanol aqueous solution with 3 g/L citric acid at rate of 1 BV/h. The concentration of anthocyanins in the desorption solution was analyzed by the UV−vis spectrophotometer.

Statistical Analysis. All of the experiments were performed in triplicate, and data are shown as mean values ± SD. Statistical analysis was done using one-way analysis of variance (ANOVA), and the mean values were considered to be significantly different when $p < 0.05$.

RESULTS AND DISCUSSION

Preselection of the Resins. Nine macroporous resins with different properties were tested through static adsorption, and the adsorption capacity (q_e) and desorption ratio (D) were used to evaluate their adsorbent efficiencies. The adsorption of macroporous resin is a physical action through van der Waals force or hydrogen bonding. According to the rule "likes dissolve likes", given roselle anthocyanins contain nonpolar phenylallyl groups and polar multihydroxy groups, either nonpolar resins or polar resins were applicable to the adsorption of roselle anthocyanins, and nine macroporous resins, ranging from nonpolarity to polarity, were therefore tested to select the appropriate resin for adsorbing and separating roselle anthocyanins in calyx extracts. Table 1 shows the physical characteristics of the adsorbent resins and their adsorption properties in increasing order. AB-8, X-5, and HPD-100 resins present relatively low adsorption capacities. Except for SP-207 and XAD-4, the amount of anthocyanins adsorbed seems to be proportional to the adsorbent surface area. Similar results have been reported by other authors.[24−27] In general, the surface area and the pore radius of the adsorbent keep a linear relationship with the adsorption capacity for resins.[28] Although SP207 and XAD-4 have relatively lower specific surface areas than those of DM-21, LS-305A, LS-610B, and LS-305, their larger pore radius may well account for their high adsorption characteristics.

As shown in Table 1, it was found that anthocyanins desorbed almost completely from AB-8, X-5, HPD-100, SP-207, and DM-21. However, desorption from XAD-4 is likely to be most difficult as compared with other resins, which might indicate the strong interaction between solute and the adsorbent material.

Considering the small adsorption capacities of AB-8, X-5, and HPD-100 and the lowest desorption ratio of XAD-4, these four resins were not adaptable as adsorbents of anthocyanins. Therefore, SP207, DM-21, LS-305A, LS-610B, and LS-305 were applied for the following study.

Static Adsorption Isotherms. Two popular theoretical models (the Langmuir and Freundlich models) are used to compare adsorption of resins.[14]

Langmuir equation:

$$q_e = \frac{q_{max} K_L C_e}{1 + K_L C_e} \quad (4)$$

Freundlich equation:

$$q_e = K_F C_e^{1/n} \quad (5)$$

q_e and C_e represent the same parameters as in eq 1, q_{max} is the maximum adsorption capacity (mg/g), K_L is the Langmuir constant, and K_F and n are the Freundlich constants.

Considering the thermal instability of roselle anthocyanins,[1,29−31] adsorption isotherms of roselle anthocyanins onto SP207, DM-21, LS-305A, LS-610B, and LS-305 resins were performed at room temperature (25 °C). From our preliminary experiments, anthocyanin-containing roselle extracts displayed their greatest stabilities at acidic pH (e.g., ≤3.0). Similar results were reported by Laleh et al.[32] and Selim et al.[18] Therefore, adsorption isotherms were carried out at pH 2.0, 2.5, and 3.0 in this study.

Figure 1 shows the adsorption isotherms of roselle anthocyanins on the resins at pH 2.0, 2.5, and 3.0. Langmuir

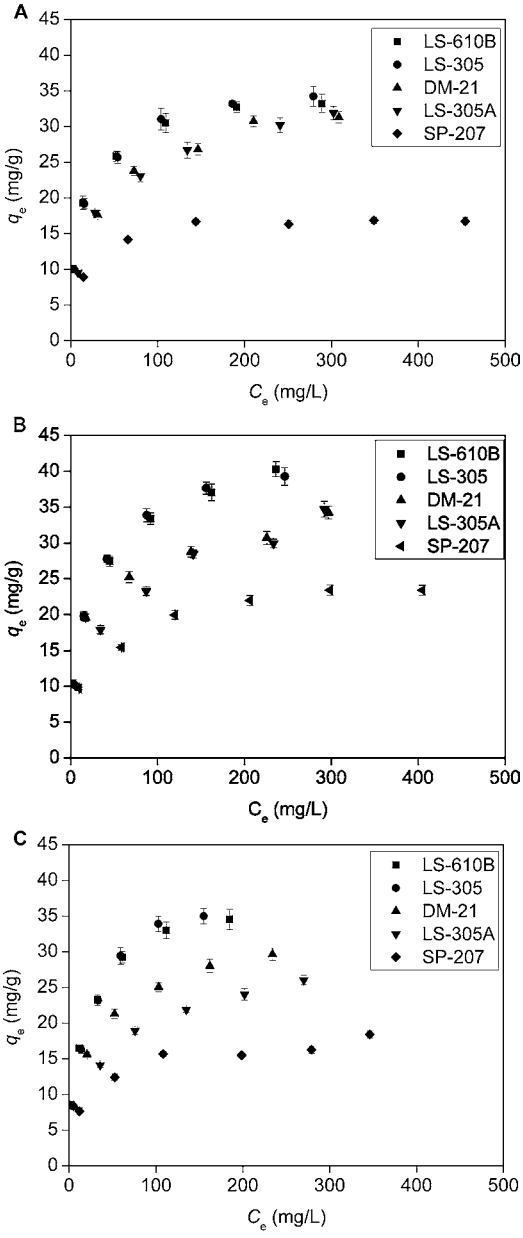

Figure 1. Adsorption isotherm at different pH values at T = 25 °C: (A) pH 2.0; (B) pH 2.5; (C) pH 3.0.

constants, q_{max} and K_L, were calculated from the linear plot of C_e/q_e versus C_e. The Freundlich constants, K_F and n, were calculated from the linear plot of log q_e versus log C_e. The experimental data were statistically analyzed, and r^2 values were obtained and are presented in Table 2. It appears that the

Table 2. Evaluated Constants for Langmuir and Freundlich Equations at 25 °C

		Langmuir equation			Freundlich equation		
resin	pH	K_L	q_{max}	r^2	K_F	n	r^2
LS-305	2.0	0.1195	32.2581	0.9881	7.8037	3.5423	0.9526
	2.5	0.0813	38.1679	0.9944	7.1829	3.0111	0.9495
	3.0	0.0539	38.0228	0.9984	4.7195	2.3175	0.9678
LS-610B	2.0	0.1838	30.5810	0.9806	8.8288	3.9479	0.9560
	2.5	0.0900	31.9489	0.9935	8.7438	3.4650	0.9929
	3.0	0.1674	30.1205	0.9666	7.0129	3.0530	0.9788
DM-21	2.0	0.1099	27.9330	0.9541	6.4953	3.4941	0.9878
	2.5	0.0900	30.8560	0.9935	7.5318	3.6805	0.9338
	3.0	0.0776	28.0112	0.9873	5.2131	2.9558	0.9730
LS-305A	2.0	0.0544	28.5714	0.9936	5.5348	3.1878	0.9443
	2.5	0.0991	30.5810	0.9410	5.7398	3.1250	0.9940
	3.0	0.0418	25.7069	0.9894	3.6000	2.7480	0.9788
SP-207	2.0	0.0731	17.4825	0.9951	6.0256	5.5127	0.8756
	2.5	0.0779	22.3714	0.9511	5.6728	4.0290	0.9803
	3.0	0.0650	17.3611	0.9792	4.4648	2.7480	0.9422

experimental points fitted well to both the Langmuir and Freundlich models. Comparison of the coefficients of determination (r^2) of the models showed the Langmuir model to be slightly better than the Freundlich one. As shown in Table 2, the maximum adsorption occurred at pH 2.5, and at this pH, the values of q_{max} (obtained from Langmuir plots) increase in the order LS-305 > LS-610B > DM-21 > LS-305A > SP-207. The most effective are LS-305 and LS-610B, which can be attributed to their highest surface areas among the resins considered. LS-305 seemed to favor higher concentration, thus resulting in the very high maximum adsorption capacity, 38.16 mg/g, at pH 2.5 (calculated from the Langmuir model). DM-21 and LS-305A show an intermediate capacity at pH 2.0 and 2.5, whereas at pH 3.0, DM-21 exhibited higher affinity than LS-305A. The worst is SP-207 owing to its small surface area, which was omitted in the following tests.

The adsorption capacity was the highest when the pH was 2.5 and decreased by either raising or lowering pH under the experimental condition. These results may be explained on the basis of the structural transformations of anthocyanins as a function of pH.[33,34] In acidic aqueous solutions anthocyanins exist as four main equilibrium species: the quinonoidal base A, the flavylium cation AH^+, the carbinol or pseudobase B, and the chalcone C. Figure 2 presents the distribution of the four main equilibrium species of malvidin 3-glucoside,[35] which is considered to be a typical example in this study for describing the relative amounts of each equilibrium form varying with both the pH value and the structure of a certain anthocyanin.[36,37]

At pH 2.0 the red flavylium cation is the mainly predominating equilibrium species; the apolar styrene–divinylbenzene resins tested here are unfavorable to the adsorption of the polar flavylium cation and thus a decreased adsorption capacity of roselle anthocyanins. Increasing the pH value to 2.5 inflicts a decrease of both the color intensity and the concentration of the flavylium cation to the colorless neutral carbinol form; an increase of adsorption capacity is presumably due to the increase of the hydrophobicity in equilibrium solution and thus enhances their adsorbability.[14] When the pH increases further to 3.0, more carbinol form is

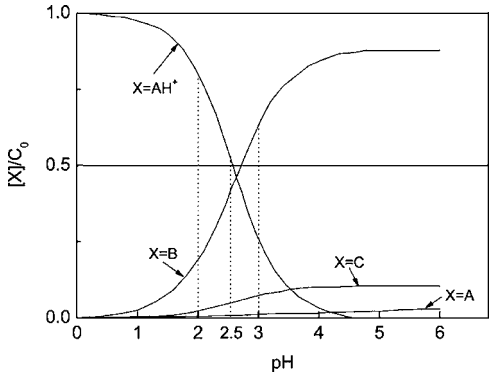

Figure 2. Distribution of the different malvidin 3-glucoside equilibrium forms according to pH: (AH^+) flavylium cation; (A) quinonoidal base; (B) carbinol or anhydrobase; (C) chalcone.

yielded through ring-opening, and more carbinol is irreversibly changed to the colorless chalcone, which does not absorb visible light.[35] Also, a rapid proton loss of the flavylium cation takes place as the pH shifts to 3.0 and the colored quinonoidal form rises. Although the transformation of flavylium cation to carbinol or anhydrobase can increase the adsorption capacity due to the decrease of polarity of the equilibrium species, it cannot compensate for the loss in adsorption capacity induced by the irreversible formation of chalcone.[35] The quinonoidal form exists in a neglectable percentage and does not affect the overall color of solution noticeably[36] or the adsorption performance of resins.

Static Desorption. Ethanol is the preferable desorbent for macroporous resin because it can be easily removed from the solution and recycled and has low cost and no toxicity to the samples.[15,38−41] In addition, acidic solutions have been used to elute anthocyanins from resins with the objective of maintaining the flavylium cation form, which is red and stable in a highly acid medium.[14,33,42] Ethanol solution acidified with citric acid instead of hydrochloric acid would be preferred for food use to avoid the poisonous residue of hydrochloric acid in the preparative pigment product. Therefore, different concen-

dx.doi.org/10.1021/jf205311v | J. Agric. Food Chem. 2012, 60, 2368−2376

trations of ethanol/citric acid solutions were used to perform desorption tests to find most suitable desorption solution. Figure 3 shows the desorption ratio of different ethanol

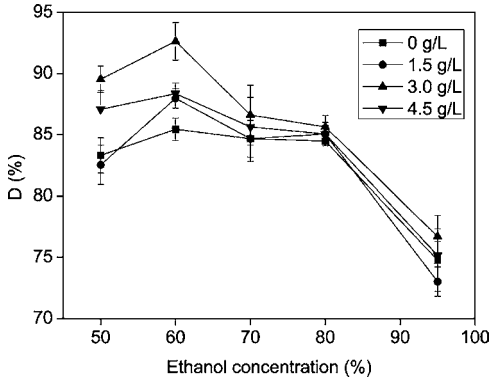

Figure 3. Effect of ethanol/citric acid concentrations on desorption ratio of LS-305 resin.

concentrations with various citric acid contents (0, 1.5, 3.0, 4.5 g/L, respectively) on LS-305 resin. As shown in Figure 3, the desorption ratio of roselle anthocyanins increased with the increase of ethanol concentration, reached its peak value at the concentration of 60%, and then sharply decreased with the increase of ethanol concentration; the worst desorption occurs at 95% ethanol concentration. On the other hand, using 3.0 g/L citric acid allows a significant increase in the desorption performance of roselle anthocyanins, especially at 60% ethanol solution. Desorption of roselle anthocyanins from macroporous resin is the result of competing interactions between the intermolecular forces of adsorption on the macroporous resin and dissolution in the solvent. When intermolecular forces are recessive, roselle anthocyanins desorb from the resin into the solvent. A 60% ethanol solution with 3.0 g/L citric acid might be the best matching of polarity between desorption solvent and adsorbate, thus facilitating desorption. Therefore, 60% ethanol solution with 3.0 g/L citric acid was selected as the optimal desorption solution and used in the dynamic desorption experiment. Similar profiles were observed for desorption of roselle anthocyanins on other resins (figures not shown). A comparison of the adsorption/desorption results for the four resins at 60% ethanol with 3.0 g/L citric acid is shown in Table 3.

Table 3. Comparison of Static Adsorption/Desorption Results for Roselle Anthocyanins on Different Resins (Desorption by 60% Ethanol Concentration with 3.0 g/L Citric Acid)

type	adsorption capacity (mg/g)	desorption ratio (%)
LS-610B	18.40 ± 0.29	85.12 ± 2.85
LS-305	18.29 ± 0.33	92.63 ± 3.14
DM-21	16.41 ± 0.25	98.40 ± 2.21
LS-305A	16.02 ± 0.39	88.90 ± 1.87

As seen in Table 3, LS-610B resin exhibited the highest adsorption capacity but the lowest desorption ratio, indicating that it possessed a strong affinity for roselle anthocyanins, as well as a considerable fraction of the small internal pores of LS-610B. A maximum desorption efficiency of >98%, using DM-21, is observed, despite a relatively low adsorption capacity. LS-305 shows an intermediate adsorption/desorption efficiency in comparison to LS-610B and DM-21, and the worst is LS-305A, which shows the least adsorption capacity and <90% of desorption ratio. In the comprehensive consideration of the adsorption capacity and desorption ratio, LS-610B, LS-305, and DM-21 were used in the following experiments.

Static Adsorption and Desorption Kinetics. Figure 4 presents the plot of roselle anthocyanins adsorbed (q_t) versus

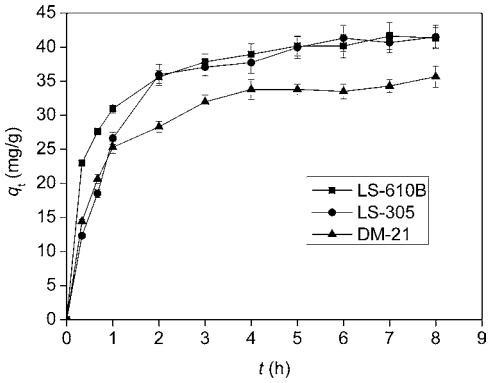

Figure 4. Adsorption kinetic curves of roselle anthocyanins onto three resins.

contact time (t) for LS-610B, LS-305, and DM-21 at 25 °C. Obviously, the equilibrium for the uptake of LS-610B, LS-305, and DM-21 was reached within 7 h.

The adsorption−time data in Figure 4 were treated according to pseudo-first-order,[43] pseudo-second-order,[44] and the intraparticle diffusion.[45]

Pseudo-first-order model:

$$\log(q_e - q_t) = \log q_e - \left(\frac{k_1 t}{2.303}\right) \quad (6)$$

Pseudo-second-order model:

$$\frac{t}{q_t} = \frac{1}{k_2 q_e^2} + \frac{t}{q_e} \quad (7)$$

Particle diffusion kinetics model:

$$q_t = X + k_p t^{1/2} \quad (8)$$

q_e and q_t are the amounts of roselle anthocyanins adsorbed onto adsorbents at equilibrium and at contact time t, respectively (mg/g), k_1 is the pseudo-first-order rate constant (h^{-1}), k_2 is the pseudo-second-order rate constant (g/mg h), k_p is the intraparticle diffusion rate constant (mg/g $h^{1/2}$), and X represents the boundary layer diffusion effects (external film resistance).

Kinetics parameters are determined and listed in Table 4. Results show that roselle anthocyanin adsorption kinetics on these three resins are best fitted by the pseudo-second-order model. This is deduced from the higher correlation coefficient values (r^2) obtained with the pseudo-second-order model, and the calculated q_e(calcd) values are closer to the experimental data than the calculated values of the pseudo-first-order model. Similar results have been reported by other authors.[23,41,46] According to the pseudo-second-order rate constant, k_2, the adsorption rate of the three reins is ordered as follows: LS-610B > DM-21 > LS-305 (Table 3).

dx.doi.org/10.1021/jf205311v | J. Agric. Food Chem. 2012, 60, 2368−2376

Table 4. Kinetic Parameters of Roselle Anthocyanins onto Three Resins at 25 °C

				pseudo-first-order model			pseudo-second-order model		
resin	q_e (exptl) (mg/g)	k_p (mg/g $h^{1/2}$)	r^2	k_1 (h^{-1})	q_e (calcd) (mg/g)	r^2	k_2 (h^{-1})	q_e (calcd) (mg/g)	r^2
LS-610B	41.61 ± 1.49	29.799	0.9637	0.4788	18.40	0.9632	0.0593	43.29	0.9995
LS-305	41.50 ± 0.97	22.439	0.8940	1.0620	74.71	0.7102	0.0275	45.87	0.9977
DM-21	35.67 ± 1.21	22.341	0.9158	0.3740	15.81	0.9095	0.0495	37.45	0.9987

The pseudo-first-order and pseudo-second-order models basically consider external film diffusion, intraparticle diffusion, and interaction step for the adsorption process. Although the particle diffusion kinetics models cannot represent the whole adsorption processes, they can be applied to give a definite mechanism of adsorption. According to Figure 5, the slope of

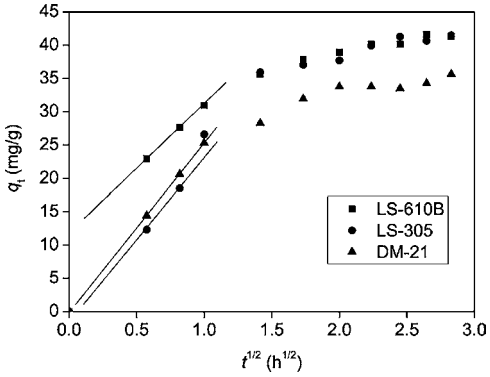

Figure 5. Intraparticle diffusion model for roselle adsorption onto three resins.

the linear part of the curve gives the initial rate of adsorption by all three resins (here taken at 1 h), controlled by intraparticle diffusion.[45,47] The positive value X for the adsorption of roselle anthocyanins on LS-610B, which is proportional to the boundary layer thickness,[45] indicates that the intraparticle diffusion is not the only rate-controlled step and the external film diffusion controls the adsorption to some degree.[41,48]

Desorption kinetics of roselle anthocyanins on LS-610B, LS-305, and DM-21 resins were investigated at 25 °C and are shown in Figure 6. As illustrated in Figure 6 compared with

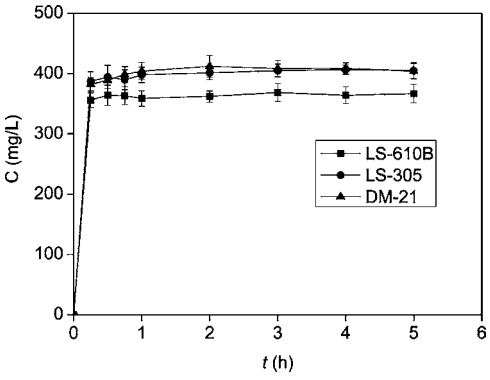

Figure 6. Desorption kinetics curves of roselle anthocyanins on three resins at 25 °C.

Figure 4, the desorption rate was much faster than the adsorption rate, the asymptotic curves were reached after 30 min of contact time, and the desorption equilibria were established for the three resins, which suggested that the bonding force between resins and roselle anthocyanins was weaker than the force between the eluant and roselle anthocyanins. It should be noted that desorption from LS-610B is obviously the most difficult as compared with LS-305 and DM-21.

Dynamic Adsorption and Elution. Figure 7 shows the experimental breakthrough curves. In general, an increasing

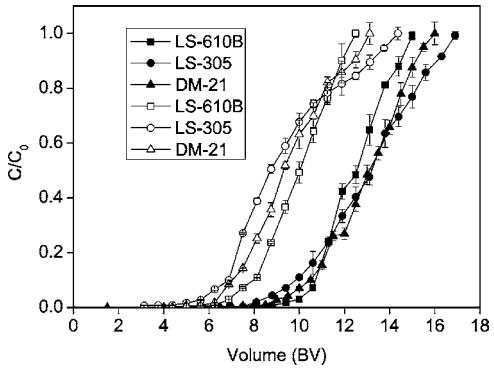

Figure 7. Dynamic breakthrough curves of roselle anthocyanins on three resins at different flow rates. Solid and open symbols represent 1 and 2 BV/h, respectively (T = 25 °C, pH 2.5, C_0 = 748.99 mg/L).

flow rate has a negative effect on the dynamic adsorption capacity of adsorbate on resins because adsorbate molecules do not have sufficient time to undergo interactions with active sites at the surface of resins and vice versa.[39] As expected, the results indicated that for higher flow rate the breakthrough time and the saturation time are achieved more quickly. The desorption parameters are listed in Table 5. As can been seen from Table

Table 5. Comparison of Dynamic Adsorption Capacities at Breakthrough and Saturation Points and Desorption Ratio of Roselle Anthocyanins on Different Resins at Flow Rates of 1 and 2 BV/h

type	flow rate (BV/h)	q_b[a] (mg/mL wet resin)	q_s[b] (mg/mL wet resin)	R[c] (%)
LS-610B	1	7.34 ± 0.18	7.75 ± 0.28	94.7
LS-305	1	6.29 ± 0.14	8.64 ± 0.19	72.8
DM-21	1	6.93 ± 0.27	8.93 ± 0.23	77.6
LS-610B	2	4.53 ± 0.17	6.05 ± 0.17	74.9
LS-305	2	4.59 ± 0.19	7.75 ± 0.09	59.2
DM-21	2	4.53 ± 0.13	7.02 ± 0.13	64.5

[a] q_b, breakthrough adsorption capacity, mg/mL wet resin. [b] q_s, saturation adsorption capacity, mg/mL wet resin. [c] R, efficiency of resin utilization = $q_b/q_s \times 100\%$.

5, LS-610B has the highest breakthrough capacity among the three resins, and also the adsorption of roselle anthocyanins on LS-610B shows the sharpest breakthrough curve among the

dx.doi.org/10.1021/jf205311v | J. Agric. Food Chem. 2012, 60, 2368−2376

three resins, indicating that LS-610B possesses the highest efficiency of resin utilization and LS-305 the lowest. Because breakthrough adsorption capacities and efficiencies of resin utilization differed significantly ($p < 0.05$) at flow rates of 1 and 2 BV/h, 1 BV/h was used as the proper adsorption flow rate.

Figure 8 shows the dynamic desorption curves of fully saturated columns on the three resins based on the volume of

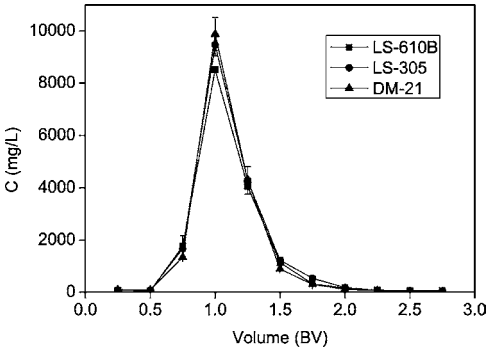

Figure 8. Dynamic desorption curves of roselle anthocyanins on three resins at a flow rate of 1 BV/h, T = 25 °C.

desorption solution and the concentration of roselle anthocyanins. Narrow and symmetric peaks with almost the same shape were observed for the three resins. The slight reduction of the elution peak for LS-610B may be due to the most difficult desorption of roselle anthocyanins from LS-610B. The desorption process of roselle anthocyanins from the three resins could be almost completed by approximately 100 mL (2.5 BV) of desorption solution.

In an actual process for separating roselle anthocyanins, the adsorption step is usually terminated when the breakthrough concentration becomes about 5% of the inlet concentration. The corresponding desorption curves will be different from those of fully saturated columns shown in Figure 8. Continuous adsorption−regeneration and desorption tests were repeated for 10 runs to test its reusability (Table 6). In this case, the adsorption test was terminated at breakpoint. The discrepancy is more pronounced for run 1 compared with run 2, the breakthrough capacities being much higher and the desorption ratios are much lower than those of run 2, whereas these data show no significant changes during the later successive cycles from runs 2−10 ($p > 0.05$), which is important for practical application. By comparison of the data obtained from runs 2−10, the desorption capacity of DM-21 was the lowest among the three resins, whereas nearly no differences between LS-610B and LS-305 were seen. The adsorbent LS-305 has a desorption capacity similar to that of LS-610B and has the highest desorption ratio, which can compensate for the decrease in adsorption capacity. For LS-610B, additional loss of roselle anthocyanins occurred in the course of water washing, probably implying that water can weaken the bonding force between LS-610B and roselle anthocyanins. In light of the considerations presented above, LS-305 was the most appropriate among the three resins for its almost complete desorption ratio with acceptable adsorption capacity.

Samples after purification by LS-305 resin were combined, concentrated under vacuum pressure, and then placed in a drying oven at 60 °C until the mass did not change. The content of roselle anthocyanins increased from 748.99 mg/L calyx extract solution to 48.53 mg/g pigment product, and the overall yield of pigment product (dry powder) was 49.6 mg/g dried calyces.

Conclusions. In the current study, the separation characteristics of nine kinds of styrene−divinylbenzene macroporous resins were systematically investigated by means of static adsorption/desorption experiments. LS-610B and LS-305 exhibited higher adsorption capacity of roselle anthocyanins from *H. sabdariffa* L. extracts than the other seven adsorbents, which resulted from larger specific surface area. On the basis of the static experimental results, it was found that the experimental data fitted best to the pseudo-second-order kinetics model and Langmuir isotherm model coupled better correlation coefficients. A 60% ethanol aqueous solution with 3.0 g/L citric acid was determined as the appropriate desorption solution.

By comparison of the further dynamic adsorption/desorption experiments using a column packed with LS-610B, LS-305, and DM-21 resins, LS-305 was selected as a suitable resin for roselle anthocyanin purification, owing to its highest desorption ratio and high adsorption capacity. This method could be utilized in large-scale production of anthocyanin purification from *H. sabdariffa* L. extracts in industry, due to the prominent advantages of the macroporous resin method such as the procedural simplicity, lower cost, lower labor intensity, higher purification efficiency, and easier scale-up.

AUTHOR INFORMATION

Corresponding Author

*Phone: +86-15105356868. Fax: +86-0535-5522090. E-mail: wenshaohong7@126.com.

Table 6. Results of the Reusability of LS-610B and LS-305 (Initial Concentration of Anthocyanins = 671.73 mg/L, T = 25 °C, pH 2.5, Flow Rate = 1 BV/h)

item	type	run 1	run 2	run 4	run 6	run 8	run 10
breakthrough capacity (mg/mL wet resin)	LS-610B	7.34 ± 0.29	6.17 ± 0.31	6.20 ± 0.15	6.08 ± 0.32	6.11 ± 0.30	6.14 ± 0.15
	LS-305	6.29 ± 0.15	5.56 ± 0.27	5.64 ± 0.18	5.45 ± 0.25	5.40 ± 0.23	5.60 ± 0.21
	DM-21	6.93 ± 0.32	5.71 ± 0.18	5.65 ± 0.27	5.68 ± 0.16	5.55 ± 0.17	5.64 ± 0.27
desorption capacity (mg/mL wet resin)	LS-610B	5.91 ± 0.15	5.47 ± 0.21	5.61 ± 0.31	5.44 ± 0.17	5.36 ± 0.16	5.55 ± 0.24
	LS-305	5.82 ± 0.33	5.52 ± 0.14	5.57 ± 0.22	5.43 ± 0.24	5.39 ± 0.18	5.54 ± 0.30
	DM-21	6.40 ± 0.18	5.09 ± 0.13	5.00 ± 0.16	5.18 ± 0.18	4.98 ± 0.22	5.19 ± 0.28
desorption ratio (%)	LS-610B	80.50 ± 2.60	88.73 ± 3.93	90.53 ± 3.60	89.47 ± 3.75	87.68 ± 3.46	90.42 ± 3.06
	LS-305	92.51 ± 3.73	99.23 ± 3.67	98.75 ± 3.53	99.68 ± 4.49	99.78 ± 3.79	98.94 ± 4.53
	DM-21	92.32 ± 3.43	89.06 ± 2.54	88.47 ± 3.53	91.24 ± 2.87	89.75 ± 3.36	90.05 ± 4.58

Funding

We gratefully acknowledge the generous support provided by Shandong Province Nature Science Fund (ZR2010BL027), Shandong Outstanding Young Scientist Award Fund (2008BS02009), and Yantai Science and Technology research project fund (2011072 and 2011455).

Notes

The authors declare no competing financial interest.

REFERENCES

(1) Chen, S. H.; Huang, T. C.; Ho, C. T.; Tsai, P. J. Extraction, analysis, and study on the volatiles in roselle tea. *J. Agric. Food Chem.* **1998**, *46*, 1101−1105.

(2) Duangmal, K.; Saicheua, B.; Sueeprasan, S. Colour evaluation of freeze-dried roselle extract as a natural food colorant in a model system of a drink. *LWT−Food Sci. Technol* **2008**, *41*, 1437−1445.

(3) Abou-Arab, A .A.; Abu-Salem, F. M.; Abou-Arab, E. A. Physico-chemical properties of natural pigments (anthocyanin) extracted from roselle calyces (*Hibiscus subdariffa*). *J. Am. Sci.* **2011**, *7*, 445−456.

(4) Lin, T. L.; Lin, H. H.; Chen, C. C.; Lin, M. C.; Chou, M. C.; Wang, C. J. *Hibiscus sabdariffa* extract reduces serum cholesterol in men and women. *Nutr. Res. (N.Y.)* **2007**, *27*, 140−145.

(5) Tsai, P. J.; McIntosh, J.; Pearce, P.; Camden, B.; Jordan, R. B. Anthocyanin and antioxidant capacity in roselle (*Hibiscus sabdariifa* L.) extract. *J. Food. Res. Int.* **2002**, *35*, 351−356.

(6) Yin, M. C.; Chao, C. Y. Anti-campylobacter, anti-aerobic, and anti-oxidative effects of roselle calyx extract and protocatechuic acid in ground beef. *Int. J. Food Microbiol.* **2008**, *127*, 73−77.

(7) Christian, K. R.; Jackson, J. C. Changes in total phenolic and monomeric anthocyanin composition and antioxidant activity of three varieties of sorrel (*Hibiscus sabdariffa*) during maturity. *J. Food Compos. Anal.* **2009**, *22*, 663−667.

(8) Christian, K. R.; Nair, M. G.; Jackson, J. C. Antioxidant and cyclooxygenase inhibitory activity of sorrel (*Hibiscus sabdariffa*). *J. Food Compos. Anal.* **2006**, *19*, 778−783.

(9) Du, C. T.; Francis, F. J. Anthocyanins of roselle (*Hibiscus sabdariffa* L.). *J. Food Sci.* **1973**, *38*, 810−812.

(10) Bridle, P.; Timberlake, C. F. Anthocyanins as natural food colours − selected aspects. *Food Chem.* **1997**, *58*, 103−109.

(11) Cissé, M.; Vaillant, F.; Bouquet, S.; Pallet, D.; Lutin, F.; Reynes, M.; Dornier, M. Athermal concentration by osmotic evaporation of roselle extract, apple and grape juices and impact on quality. Innov. *Food Sci. Emerg. Technol* **2011**, *12*, 352−360.

(12) Cissé, M.; Vaillant, F.; Pallet, D.; Dornier, M. Selecting ultrafiltration and nanofiltration membranes to concentrate anthocyanins from roselle extract (*Hibiscus sabdariffa* L.). *Food Res. Int.* **2011**, *9*, 2607−2614.

(13) Scordino, M.; Di Mauro, A.; Passerini, A.; Maccarone, E. Adsorption of flavonoids on resins: cyanidin 3-glucoside. *J. Agric. Food Chem.* **2004**, *52*, 1965−1972.

(14) Mauro, A.; Arena, E.; Fallico, B.; Passerini, A.; Maccarone, E. Recovery of anthocyanins from pulp wash of pigmented oranges by concentration on resins. *J. Agric. Food Chem.* **2002**, *50*, 5968−5974.

(15) Cao, S. Q.; Pan, S. Y.; Yao, X. L.; Fu, H. F. Isolation and purification of anthocyanins from blood oranges by column chromatography. *Agr. Sci. China* **2010**, *9*, 207−215.

(16) Matsumoto, H.; Hanamura, S.; Kawakami, T.; Sato, Y.; Hirayama, M. Preparative-scale isolation of four anthocyanin components of black currant (*Ribes nigrum* L.) fruits. *J. Agric. Food Chem.* **2001**, *49*, 1541−1545.

(17) Gradinaru, G.; Biliaderis, C. G.; Kallithrakac, S.; Kefalas, P.; Garcia-Viguera, C. Thermal stability of *Hibiscus sabdariffa* L. anthocyanins in solution and in solid state: effects of copigmentation and glass transition. *Food Chem.* **2003**, *83*, 423−436.

(18) Selim, K. A.; Khalil, K. E.; Abdel-Bary, M. S.; Abdel-Azeim, N. A. Extraction, encapsulation and utilization of red pigments from Roselle (*Hibiscus sabdariffa* L.) as natural food colourants. *Alex. J. Food Sci. Technol. (Special Vol. Conf.)* **2008**, 7−20.

(19) Lee, J.; Durst, R. W.; Wrolstad, R. E. Determination of total monomeric anthocyanin pigment content of fruit juices, beverages, natural colorants, and wines by the pH differential method: collaborative study. *J. AOAC Int.* **2005**, *88*, 1269−1278.

(20) Cissé, M.; Vaillant, F.; Acosta, O.; Dhuique-Mayer, C.; Dornier, M. Thermal degradation kinetics of anthocyanins from blood orange, blackberry, and roselle using the Arrhenius, Eyring, and Ball models. *J. Agric. Food. Chem.* **2009**, *57*, 6285−6291.

(21) Cissé, M.; Vaillant, F.; Soro, D.; Reynes, M.; Dornier, M. Crossflow microfiltration for the cold stabilization of roselle (*Hibiscus sabdariffa* L.) extract. *J. Food Eng.* **2011**, *106*, 20−27.

(22) Cai, J. G.; Li, A. M.; Shi, H. Y.; Fei, Z. H.; Long, C.; Zhang, Q. X. Adsorption characteristics of aniline and 4-methylaniline onto bifunctional polymeric adsorbent modified by sulfonic groups. *J. Hazard. Mater. B* **2005**, *124*, 173−180.

(23) Zeng, X. W.; Fan, Y. G.; Wu, G. L.; Wang, C. H.; Shi, R. F. Enhanced adsorption of phenol from water by a novel polar post-crosslinked polymeric adsorbent. *J. Hazard. Mater.* **2009**, *169*, 1022−1028.

(24) Jogdeo, D. A.; Niranjan, K.; Pangarkar, V. G. Recovery of dissolved allyl isothiocyanate from mustard essential oil steam distillation condensate. *J. Chem. Technol. Biotechnol.* **2000**, *75*, 673−680.

(25) Amin, L. P.; Pangarkar, V. G.; Beenackers, A. A. C. M. Recovery of valuable perfumery compounds from geranium steam distillation condensate using polymeric adsorbents. *Sep. Sci. Technol.* **2001**, *36*, 3639−3655.

(26) Khachane, P. K.; Heesink, A. B. M.; Versteeg, G. F.; Pangarkar, V. G. Adsorptive separation and recovery of organic compounds from purified terephthalic acid plant effluent. *Sep. Sci. Technol.* **2003**, *38*, 93−111.

(27) Deosarkar, S. P.; Pangarkar, V. G. Adsorptive separation and recovery of organics from PHBA and SA plant effluents. *Sep. Purif. Technol.* **2004**, *38*, 241−254.

(28) Scordino, M.; Mauro, A. D.; Passerini, A.; Maccarone, E. Adsorption of flavonoids on resins: hesperidin. *J. Agric. Food Chem.* **2003**, *51*, 6998−7004.

(29) Pouget, M. P.; Vennat, B.; Lejeune, B.; Pourrat, A. Extraction, analysis and study of the stability of *Hibiscus* anthocyanins. *Lebensm.-Wiss. Technol.* **1990**, *23*, 103−105.

(30) Tsai, P. J.; Huang, H. P. Effect of polymerization on the antioxidant capacity of anthocyanins in roselle. *Food Res. Int.* **2004**, *37*, 313−318.

(31) Mourtzinos, I.; Makris, D. P.; Yannakopoulou, K.; Kalogeropoulos, N.; Michali, I.; Karathanos, V. T. Thermal stability of anthocyanin extract of *Hibiscus sabdariffa* L. in the presence of *β*-cyclodextrin. *J. Agric. Food Chem.* **2008**, *56*, 10303−10310.

(32) Laleh, G. H.; Frydoonfar, H.; Heidary, R.; Jameei, R.; Zare, S. The effect of light, temperature, pH and species on stability of anthocyanin pigments in four *Berberis* species. *Pak. J. Nutr.* **2006**, *5*, 90−92.

(33) Timberlake, C. F.; Bridle, B. Anthocyanins. In *Developments in Food Colours—1*; Walford, J., Ed.; Applied Science Publishers: London, U.K., 1980; pp 115−149.

(34) Von Elbe, J. H.; Schwartz, S. J. Colourants. In *Food Chemistry*, 3rd ed.; Fennema, O. R., Ed.; Dekker: New York, 1996; pp 681−722.

(35) Brouillard, R. Chemical structure of anthocyanins. In *Anthocyanins as Food Colours*; Markakis, P., Ed.; Academic Press: London, U.K., 1982; pp 1−40.

(36) Jackman, R. L.; Yada, R. Y.; Tung, M. A.; Speers, R. A. Anthocyanins as food colorants − a review. *J. Food Biochem.* **1987**, *11*, 201−247.

(37) Mazza, G.; Brouillard, R. Colour stability and structural transformations of cyanidin 3,5-diglycoside and four 3-deoxyanthocyanins in aqueous solutions. *J. Agric. Food Chem.* **1987**, *35*, 422−426.

(38) Fan, M. H.; Xu, S. Y. Adsorption and desorption properties of macroreticular resins for salidroside from *Rhodiola sachalinensis* A. Bor. *Sep. Purif. Technol.* **2008**, *61*, 211−216.

(39) Ma, C. Y.; Tao, G. J.; Tang, J.; Lou, Z. X.; Wang, H. X.; Gu, X. H.; Hu, L. M.; Yin, M. L. Preparative separation and purification of rosavin in *Rhodiola rosea* by macroporous adsorption resins. *Sep. Purif. Technol.* **2009**, *69*, 22−28.
(40) Zhang, Y. L.; Yin, C. P.; Kong, L. C.; Jiang, D. H. Extraction optimization, purification and major antioxidant component of red pigments extracted from *Camellia japonica*. *Food Chem.* **2011**, *129*, 660−664.
(41) Lin, L. Z.; Zhao, H. F.; Dong, Y.; Yang, B.; Zhao, M. M. Macroporous resin purification behavior of phenolics and rosmarinic acid from *Rabdosia serra* (MAXIM.) HARA leaf. *Food Chem.* **2012**, *130*, 417−424.
(42) Calvarano, M.; Postorino, E.; Calvarano, I.; Gionfriddo, F. Recupero di antocianine dai residui della lavorazione delle arance pigmentate. *Essent. Der. Agrum.* **1995**, *65*, 557−566.
(43) Lagergren, S. *Zur Theorie der Sogenannten Adsorption Geloster Stoffe*; Kungliga Svenska Vetenskapsakademiens: Handlingar, Germany, 1898; pp 1−39.
(44) Ho, Y. S.; McKay, G. Pseudo-second order model for sorption processes. *Process Biochem.* **1999**, *34*, 451−465.
(45) Guibal, E.; Milot, C. J.; Tobin, M. Metal−anion sorption by chitosan beads: equilibrium and kinetic studies. *Ind. Eng. Chem. Res.* **1998**, *37*, 1454−1463.
(46) Wawrzkiewicz, M.; Hubicki, Z. Equilibrium and kinetic studies on the sorption of acidic dye by macroporous anion exchanger. *Chem. Eng. J.* **2010**, *157*, 29−34.
(47) McKay, G.; Poots, V. J. Kinetics and diffusion processes in colour removal from effluent using wood as an adsorbent. *J. Chem. Technol. Biotechnol.* **1980**, *30*, 279−292.
(48) Lorenc-Grabowska, E.; Gryglewicz, G. Adsorption of lignite-derived humic acids on coal-based mesoporous activated carbons. *J. Colloid Interface Sci.* **2005**, *284*, 416−423.